TESTING AND MODELLING OF THE ANGULAR-DEPENDENT SOLAR HEAT GAIN OF GLAZING WITH VENETIAN BLIND SHADING

H. SIMMLER*, B. BINDER

Swiss Federal Laboratories for Materials Testing and Research (EMPA)
Laboratory for Applied Physics in Building
Ueberlandstrasse 129
CH-8600 Duebendorf
Switzerland
* corresponding author, Tel: +41 1 823 5511, Fax: +41 1 823 4009, e-mail: hans.simmler@empa.ch.

ABSTRACT

As overheating problems in glassy buildings came up more and more, EMPA put a focus on the determination and modelling of the total solar energy transmittance (TSET) of multiple glazing combined with different shading systems within the framework of IEA Task 27 "Performance, durability and sustainability of solar façade components". Experimental data were produced by a calorimetric outdoor test facility near Zurich (Switzerland). In a first stage, average constant TSET values related to the incident global solar radiation were identified for a various configurations and a measuring period of a few days each. As expected the results strongly depend on the slat tilt angle as well as on the solar reflectance of the slat surface. Naturally the solar transmittance of an angle-selective component like a Venetian blind also depends on the directional distribution of the incident radiation, in particular on the sun elevation projected into the plane perpendicular to the slat rotation axis. Therefore, results from different measuring periods of the identical shading-glazing configuration are compared, and an extension of the usual average g-value identification is shown.
The experimental results are also compared with weighted average g-values from numerical modeling, which is based on a view factor method extended for circular slats in a louver type shading device. In general the agreement between measured and calculated results is good. Some deviation is explained by a significant non-diffuse Albedo component in the hemispherical radiation field. In another paper it was shown that the simplified convective heat transfer calculation used in this model may fail for mechanically ventilated double envelope façades.

Keywords: Overheating, total solar heat gain, glazing, shading, system identification, view factor method, double envelope façade

1. INTRODUCTION

Since transparent areas in the building envelope are growing continuously, high cooling energy demand and thermal comfort problems became more and more serious in the last 10 to 15 years. Both optimal energy performance and prevention of overheating in buildings require detailed knowledge of the solar transmission properties of transparent façade components, especially if the performance is expected to be "at the limit" i.e. for architectural reasons. Unfortunately there is often a lack of information in the design phase, because the behaviour of the particular façade concept is unknown, neither by measurement nor by a verified numerical model. In order to characterize and optimize the thermal and solar properties of façade components on a one-by-one scale, a calorimetric outdoor test facility was set up at the EMPA campus near Zurich (Switzerland) [1]. The test cell is a lightweight airtight PU sandwich construction surrounded by temperature controlled air in a well insulated wood frame building (Fig. 1). Just the south oriented test face is exposed to the environment. By means of a cooling system the test cell can be run at a nearly constant temperature with very little heat flux through the walls except for the test face. Therefore it is possible to run and evaluate measurements on lightweight façade components under a quasi-constant test cell temperature with little impact of test cell dynamics. Based on the measured cooling power, incident solar radiation and temperatures the total solar

energy transmittance (TSET, g-value) of a lightweight façade component can be identified after a reasonably short measuring period.
In the actual work, performed within a project in IEA Task 27 [2], a limited number of louver type shading devices in combination with insulating glazing were investigated in more detail. In the following, standard evaluation of measurements is shown for various slat colours and tilt angles. Because of the strong angular dependence of the shading transmittance it is obvious that an identified single g-value will be influenced by the range of solar incidence angles during the measuring period. For a reference case, comparisons between different measuring periods (seasonal effects) and results from more detailed identification models are presented and discussed. The experimental results are compared with numerical calculations based on a view factor method [3] that was extended for lamellae with circular shape.

Figure 1. EMPA outdoor test facility. Two test cells are built in a wooden building. Temperature controlled indoor air is flowing around the cell walls except for the test face which is exposed to the environment. Climate data sensors including a tracker for direct normal radiation are located between the two test faces.

In addition a mechanically ventilated glass double façade with integrated shading was measured and analyzed by means of a coupled thermal - fluid mechanical model. These results are reported in a separate publication [4].

2. EXPERIMENTAL SET-UP

The experimental set-up is shown schematically in Fig. 2. A double-pane insulating glazing unit (IGU) was installed in a highly insulated surround panel, the outside glazing surface nearly flush with the exterior surface of the surround panel. The installation follows the recommendations given in IEA Task 27 to minimize shading effects by the surround panel [5]. The properties of the slight solar control glazing are:

Outside:	Sunstop Combi Neutral, 6 mm
	Solar protective, low-ε coating on surface 2
Gap:	16 mm, argon 90 %
Inside:	float glass 6 mm
Glazing area:	1.50 m x 1.25 m, including edge
	1.45 m x 1.20 m = 1.74 m^2, transparent area A after mounting
U-value:	1.2 W/m^2K, UA = 2.1 W/K
g-value:	47 % at normal incidence, gA = 0.82 m^2

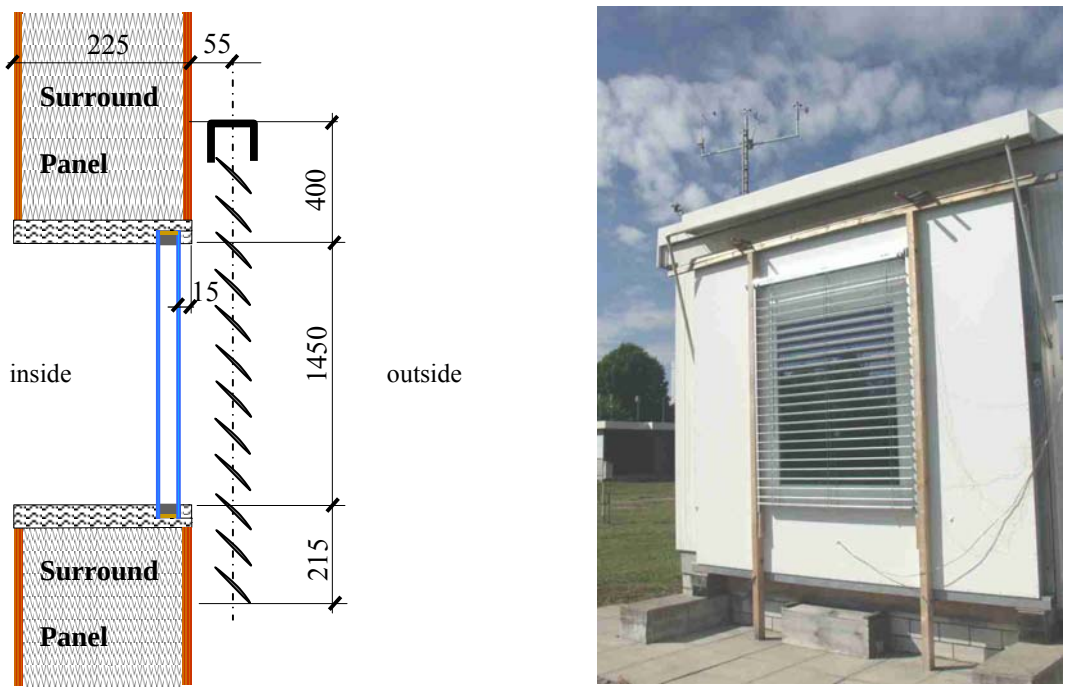

Figure 2. Vertical section through the mounted glazing and the external shading device (left). Right: view of the test frame with the mounted shading during a measuring period.

Details of the installation of the Venetian blind are indicated also in Fig. 2. The pivot of the slat is placed 70 mm in front of the exterior surface of the glazing. To prevent lateral effects with large solar incidence angles an overlap between slats and frame of about 200 mm was included around the glazing.
The shading device consists of painted profiled aluminium slats shown in Fig. 3. Major properties are:

Width:	90 mm
Vertical distance:	80 mm
Surface:	white (ρ_e = 70%), brown (ρ_e = 7%), white perforated (5% hole area fraction). The perforation allows for visible contact to the outside also in the closed position.

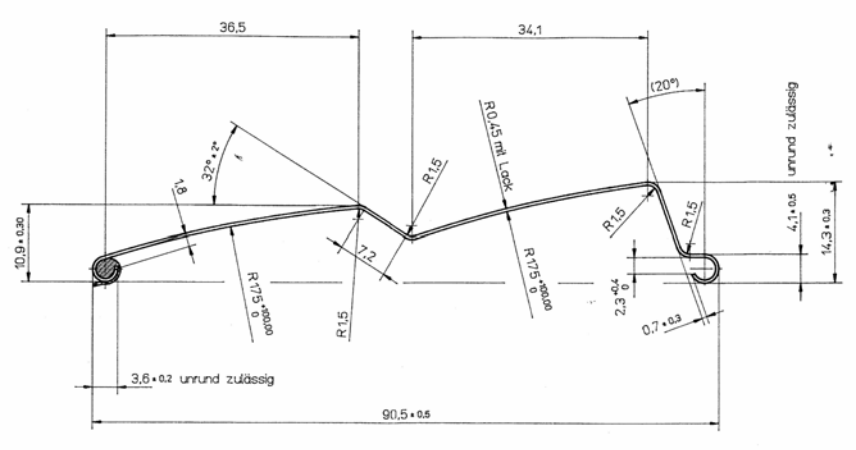

Figure 3. Cross section of the aluminium slat (left) and definition of the slat tilt angle used in this paper (right).

3. MODELING OF SOLAR RADIATION AND HEAT TRANSMISSION

The total solar energy transmittance of a partially transparent layer structure

$$g = \tau_e + q_i \qquad (1)$$

consists of the average transmittance τ_e for a standard solar radiation source and the secondary heat gain q_i that is the inward flowing fraction of the solar energy absorbed in the whole structure. The standardized calculation scheme for multiple glazing [6] is not directly applicable for the system glazing – louver type shading, since radiation as well as heat transfer through the non-planar, air permeable shading structure is not covered by the algorithms. Today several (draft) standards exist, which include the effects of a louver type shading device in a more or less simplified way [7, 3]. In the detailed procedure [3] equivalent optical layer properties of a rhomboid slat structure are calculated by means of a view factor method assuming Lambertian-diffuse surface reflectance [8]. While this requirement is well fulfilled for most surfaces, the assumption of planar slats of zero thickness causes major deviations for beam directions nearly parallel to the slat surface. Limitations may be avoided by time consuming ray-tracing calculation [9].

As an extension of the standard calculation [3] the numerical model WinSim developed at EMPA deals with view factors for circular shape of the lamella (Fig. 4). The tool calculates the optical and thermal properties of the shading and the whole layer structure as a function of solar incidence angle and slat tilt angle similar to a multiple glazing. Buoyancy driven ventilation and heat exchange around the shading layer is taken into account by a simplified piston flow model according to [3]. Air permeability of the shading is omitted.

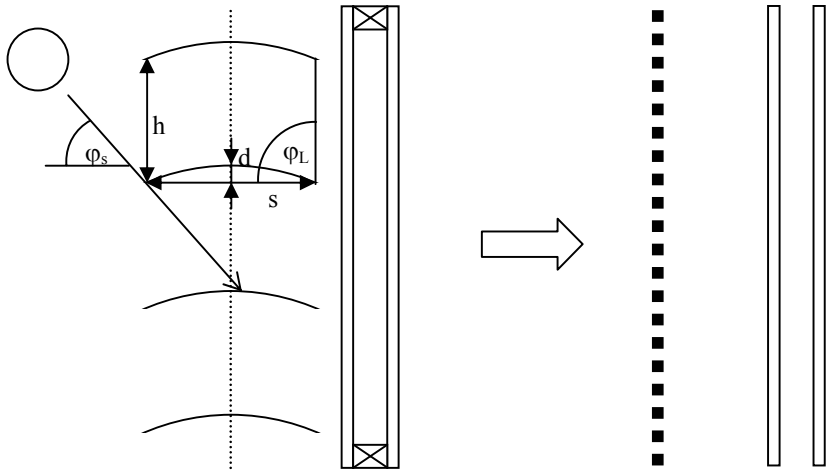

Figure 4. Geometric data of the louver type shading model and its conversion into a layer model by calculation of equivalent layer properties.

As an example the calculated g-value of the experimental configuration described in the last section with white horizontal lamellae is displayed in Fig. 5 as a function of solar height in the window direction. Negative angles apply for Albedo radiation from the ground. In contrast to the calculation with planar slats the function is no longer symmetric with respect to zero (incidence parallel to the slat). A clear difference between the g-values is seen also around zero. The deviation would be even larger for lower surface reflectance.

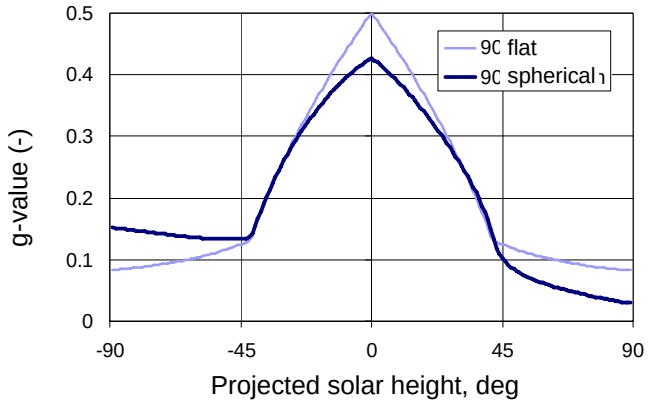

Figure 5. g-values of an insulating glazing unit with white exterior shading (c.f. experimental set-up) with horizontal slat position as a function of the solar height.

In Fig. 6 the monthly variation of the intensity weighted solar beam transmittance and the g-value is shown for the same IGU with the white shading device (horizontal slats). The climate data are hourly values of a design reference year for Zurich SMA (Switzerland). The diffuse radiation on the vertical façade plane D_v was estimated on the basis of a simplified approach [10]:

$$D_v = \frac{1}{2}\left(D_h + G_h A_g\right) \tag{2}$$

Used here are the diffuse horizontal component D_h, the global horizontal component G_h, and the Albedo A_g (set to 0.2). Whereas the solar beam transmittance varies strongly over the year, the global g-value including direct and hemispherical component is much more constant especially between March and October.

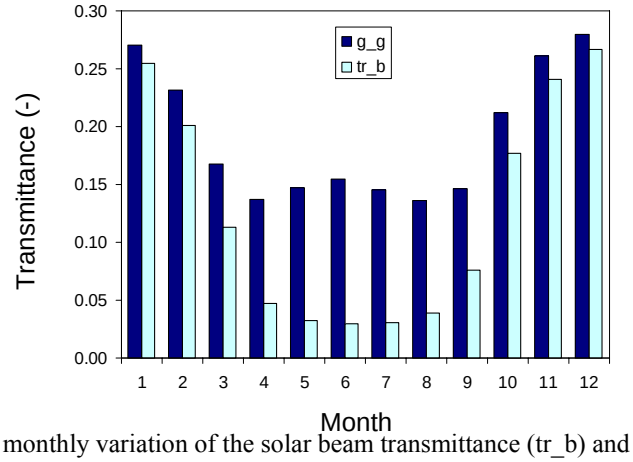

Figure 6. Calculated monthly variation of the solar beam transmittance (tr_b) and the global g-value (g_g) for south orientation in Zurich (Switzerland). Glazing and shading are similar as in Figure 5.

5. AVERAGE TSET IDENTIFICATION MODEL AND RESULTS

The thermal network model shown in Fig. 7 was used for the identification of an average solar heat gain factor in the experimental data [11]. A single potential divider (node 4) represents the test component between test cell air (node 1) and exterior air (node 5). The solar input G_vA (global vertical solar irradiation times area) is linked to node 4. A small parallel conductance H1-10 accounts for a lateral heat flow to the environment through the wooden surface layer of the test frame. Since the temperature of the service room air (node 3) around the test cell is quite homogeneous and close to the test cell temperature the test cell walls can be taken into account just by another potential divider between node 1 and node 3. The parameters not related to the test component were determined in advance by detailed calibration procedures within the IQ-TEST project [12]. The component parameters were evaluated by means of the thermal network identification software LORD [13].

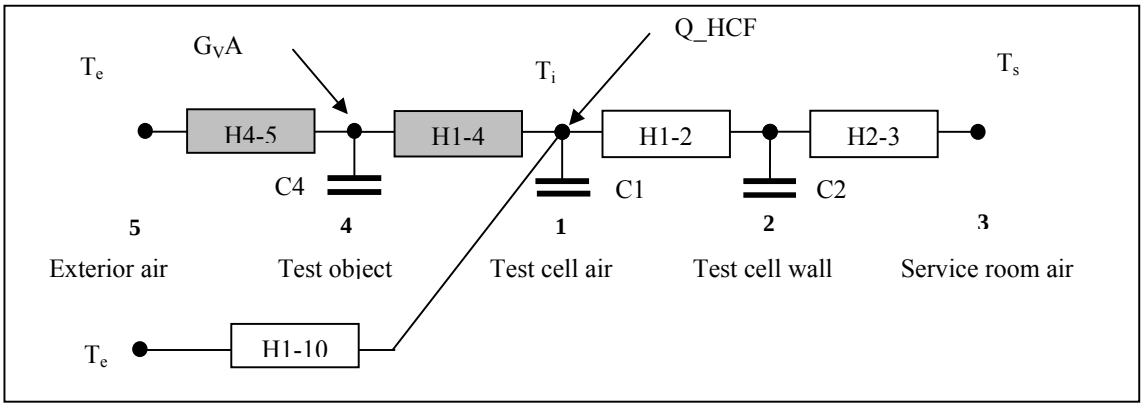

Figure 7. Thermal network model used for the basic analysis. Q_HCF is the sum of heating power, cooling power and heat flow through the surround panel. More details are described in the text.

Three types of shading devices (white, brown, white perforated) with identical slat geometry were measured for three different slat tilt angles. As the measuring periods for the non-closed slat positions are within a few weeks, the results can be assigned mainly to the characteristics of the shading device. The g-values are summarized for comparison in Table 2.

Table 2. g-value of the insulating glazing with different external shading devices as described in the text.

Slat angle	g-value (-) for slat colour		
	white	brown	white perforated
Closed	0.009	0.035	0.040
45°	0.067	0.039	0.071
90° (horizontal)	0.155	0.100	0.125

As expected the solar gain strongly depends on the slat position as well as on the slat type. The white slat shows the most dynamic behaviour: the gain is almost zero in the closed position because of the large reflectance. In the horizontal position the gain is rather high due to the light-guide capability of the white surface. The brown slat gives clearly a higher gain than the white type in the closed state, caused by a larger secondary heat gain through the hot absorbing surface. In the non-closed positions the gain is lower compared to the white slat because of the missing light-guide effect. For the "view-through" white slat a non-negligible gain has to be accepted in the closed position. In the horizontal position however the solar gain is lower than with the non-perforated white slat, explained by the reduced reflectance of the patterned surface.

Using black embrasures and a vented dark absorber surface behind the glazing a solar gain g = 0.385 was determined for the bare glazing in the beginning of July. This is about 15 % less than declared by the manufacturer for normal incidence, which is a reasonable reduction factor for hemispherical and direct radiation at about 60°-incidence angle.

In order to estimate the influence of the varying average sun elevation in different measurement periods, the most critical configuration with white slats at 90° (horizontal) was measured three times between March and June 2003. Because of small temperature differences in May and June a fixed U-value was used in all identification runs. The results are listed in Tab. 3. A relative decrease of the average solar gain of about 13 % is observed. As indicated by the model calculation (Fig. 6) the effect is not too large. Reasons are:

i) For a shading device with horizontal slat rotation axis the sun elevation projected to the window direction determines the transmittance of the shading. During maximum irradiation in the window plane (early afternoon at EMPA) the projected elevation is in the range from 40° to 60°, i.e. only a minor fraction of the whole angular range contributes to the identified solar heat gain.
ii) The angular distribution of the diffuse sky and Albedo fraction is rather independent from the measurement period. Thus the impact of the period dependent direct radiation fraction is further reduced.
We conclude that in a practical sense the radiation environment for our test site does not change too much between spring and autumn in this case. The results reasonably represent the average solar heat gain in an approximately hemispherical radiation distribution.

Table 3. Results for the white shading device with horizontal slats measured in March, May and June.

Slat position	UA (W/K)	average global g (-)	measurement period	
			from:	to:
horizontal	2.1	0.155 ± 1.1 %	11.3.03	21.3.03
horizontal	2.1	0.147 ± 3.2 %	06.5.03	27.5.03
horizontal	2.1	0.136 ± 7.4 %	06.6.03	20.6.03

An even smaller seasonal effect was expected for the slat angle 45° because only reflected radiation enters the test cell. The analysis yielded g = 0.07 for middle of March, but g = 0.09 for middle of July. That is, the solar gain is 25 % lower in March than in July! Assuming a technical problem at first, it could be observed by eye that in July the test cell inside was brighter with the 45° than with the 90° slat position an sunny days. The light grey concrete slabs in front of the test wall reflected solar beam radiation into the test cell in periods with high solar intensity. The lesson learned is that ground reflection must be taken into account in particular with angle-selective devices, for instance by adjusting the reflectance of the ground in front of the test wall and / or by measuring the Albedo part separately.

6. EVALUATION OF AN ANGLE-DEPENDENT TSET

The evaluation of an average global g-value, which is influenced by the actual boundary conditions, is a rather strong simplification. The angular selectivity of louver type shading obviously causes a strong dependence between the directional distribution of the incident solar radiation and the effective TSET. Therefore the direct and non-direct radiation components must be separated and linked to different component properties. The model and the decomposed radiation quantities are shown in Figure 8.

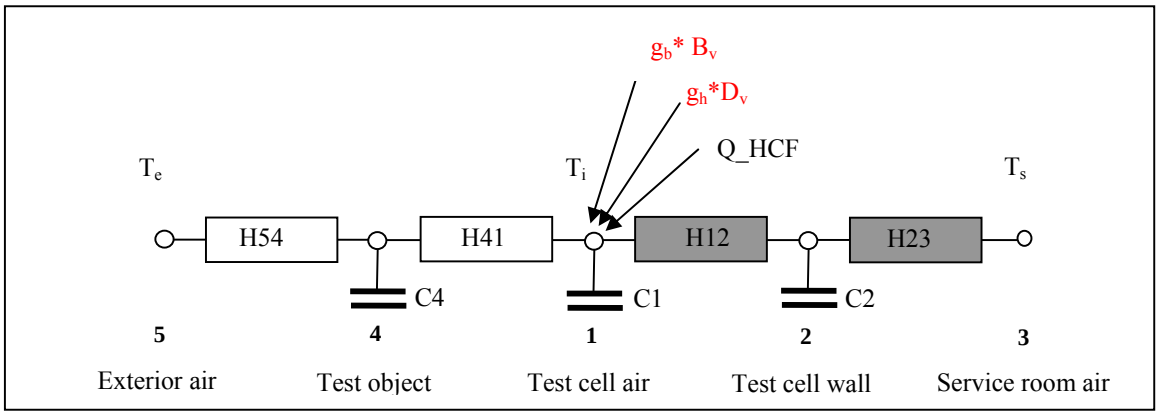

Figure 8. Thermal network model and input of the solar radiation components for a more detailed analysis of the angle dependent solar heat gain through the shading.

During the selected sunny period, the non-direct component was only a small fraction of the global irradiation on the shading plane. Therefore we focus the evaluation on the direct component, measured with a pyrheliometer on a computer-controlled tracker.

Radiation components and g-values were split as follows:

$$g_g \cdot G_v = g_b \cdot B_v + g_h \cdot D_v \qquad (3)$$

Here B_v is the direct and D_v is the diffuse radiation component in the window plane, both multiplied with respective g-values to be determined. In reality the g-value for the direct component changes dynamically with the sun elevation projected into the vertical plane in the window direction. In a certain range of incidence angles the slat structure is partly transparent to solar radiation (Fig. 9). A second fraction of (multiple) reflected radiation is transmitted also at larger incidence angles. An attempt to such an analysis has been made on data from white, horizontal lamellae taken around middle of March, where direct transmittance occurs for a few hours at the test site.

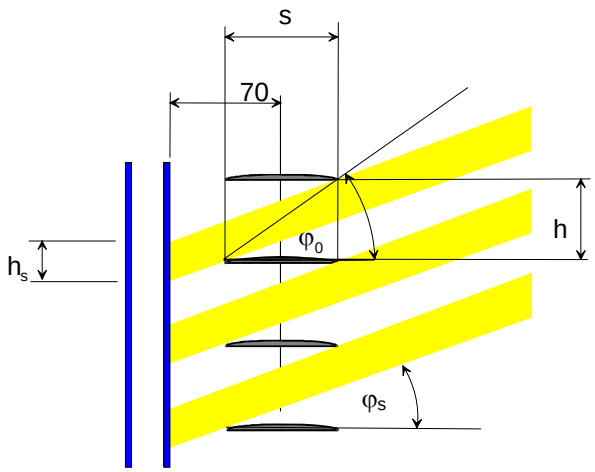

Figure 9. Left: Geometric sketch of the transmitted portion of direct solar radiation. No radiation is directly transmitted when the projected elevation angle φ is larger than φ_0, which is about 45° in our case.

Based on geometric considerations the following simplified angular dependence for the direct total solar energy transmittance was assumed:

$$g_b \approx a \cdot f(\varphi, \varphi_0) + b \cdot g(\varphi, \varphi_0) \qquad (4)$$

where *a* and *b* are constants to be identified and

$$f \approx h_s / h = 1 - \frac{w}{h} \cdot \tan(\varphi) = 1 - \frac{\tan(\varphi)}{\tan(\varphi_0)} \approx 1 - \frac{\varphi}{\varphi_0} \quad \text{for } (0 \le \varphi < \varphi_0), \text{ otherwise } f = 0 \qquad (5)$$

$$g = \frac{1 - \varphi/(\pi/2)}{1 - \varphi_0/(\pi/2)} \quad \text{for } (\varphi \ge \varphi_0), \text{ otherwise } g = 1 \qquad (6)$$

A simplified function consisting of two linear sections with a different slope is suggested also by the numerical model described before (c.f. Fig. 5).

The result of the identification is shown in Fig. 10. The cooling power peaks measured during the hours with a directly transmitted portion of the solar irradiation are missed if the basic model (single global g-value) is used, but they are well reproduced with the model involving an angle-dependent gain.

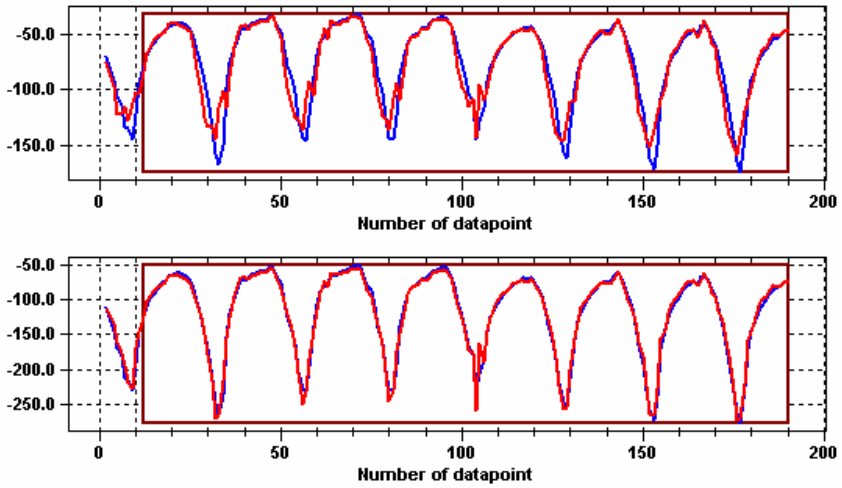

Figure 10. Quality of the cooling power fit using the basic average TSET model (top) and the extended model described in the text (bottom).

Accordingly the residual at the end of the identification process is significantly lower with the extended model. The result is now a simplified angular function for the solar heat gain

$$g_b = 0.363\left(1 - \varphi/\varphi_0\right) + 0.078 \qquad (7)$$

in the range $0 \le \varphi \le \varphi_0$. The (mathematical) uncertainty of the parameters is below 3 %. The value for $\varphi = 0$ is compared with results from other methods in Table 4.

Table 4. Total solar energy transmittance of low-ε glazing with horizontal white slats for normal incidence, determined by various methods.

Method	Remarks	g_{direct} ($\varphi = 0$)
Measurement outdoor EMPA	Identification result Equation 4	0.441
Numerical model EMPA	Glazing + shading model (cylindrical shape) solar band [14]	0.427
Measurement laboratory ISE	Calorimetric broadband measurement with solar simulator [15]	0.421
Numerical model ISE	Glazing + shading model (cylindrical shape) spectral integration [15]	0.420
Simplified calculation	EN 13363-1, $\tau_{blind} = 0.85$, treated like a screen	0.476

The agreement between the identified normal incidence g-value and various other results for this example is quite good. The exact shape of the lamella is not critical even with the complex geometry of the investigated device [15]. Rather off is a simplified calculation according to EN 13363-1 [7]. In this case, which is on the safe side, heat removal by the vented gap between shading and glazing is underestimated.

7. COMPARISON OF MEASURED AND MODELED AVERAGE g-VALUES

As mentioned before direct comparison of measured and modelled average g-values is not simple because the directional distribution of the non-beam incident radiation is basically unknown. In our measurements the relatively high reflecting concrete slabs in front of the test façades turned out to be a dominant part of the hemispherical radiation on sunny days, as described before.

The assumption of a diffuse distribution of the non-beam fraction of the incident radiation is therefore not correct. Because this major source is located vertically about -45° to -50° from the window normal, the result will be an overestimation of the solar gain in case of a horizontal slat position. If a localization of the non-beam radiation fraction is taken into account, the average g-value is in good agreement with the measured values for a weighting factor of three by one for a localized compared to a diffuse component respectively (Table 5).

Table 5. Comparison of measured and calculated weighted average g-values of an exterior shading device with a double pane IGU.

Shading	g-value		
	Calculation (diffuse)	Calculation (non-diffuse)	Outdoor testing
White, horizontal	0.20	0.17	0.16
Brown, horizontal	0.12	0.09	0.10

Another comparison was done on the same glazing and a room-side louver type shading device with the following properties: solar reflectance 71 % (white), slat width 25 mm, bending 2 mm, vertical distance 22 mm. The glazing was mounted flush with the inside surface of the test cell. It was placed with an air gap of 70 mm between glazing and slat pivot. In the closed position two options for convective heat exchange with the room were tested: i) gap blocked on top and on both sides, ii) gap fully open (free hanging shading device). The identified g-values together with weighted average calculation results are summarized in Table 6. In general good agreement can be observed. A somewhat lower experimental TSET, especially seen with the unshaded glazing, may come from a shading effect of the embrasures. The impact of a non-diffuse component in the hemispherical radiation distribution is less significant for this configuration.

Table 6. Comparison of measured and calculated weighted average g-values of an interior shading device with a double pane IGU.

Shading condition	g-value	
	Outdoor testing	Calculation
Without shading	0.39	0.41
Horizontal	0.32	0.33
45°	0.28	0.28
Closed (ca. 20°), maximum convection	0.25	0.26
Closed (ca. 20°), blocked convection	0.23	0.24

The effect of blocked or free convection between shading gap and room can be identified from the data. The change of the g-value is about 0.02 in the measurement as well as in the calculation. Last but not least it should be noted that the measured g-values are above the recommended range even with closed shading and with the well highly lamella surface present in the actual measurements.

8. CONCLUSIONS

The solar heat gain of a number of shading-glazing combinations was determined in an outdoor test facility. The performance in the real situation clearly shows the influence of shading characteristics like surface color and tilt angle. Seasonal effects due to the changing radiation environment, especially the average sun elevation, can be estimated as well. Between spring and midsummer these effects are not too serious with regard to the global weighted average g-value of a shaded glazing system. For one configuration the angular dependence of the solar heat gain was identified by means of a parameterized function. Good agreement between those results and other methods was obtained.

Calculated weighted average g-values based on optical modelling of lamellae with circular shape and diffuse surface reflectance are in good correspondence with global solar heat gains extracted from outdoor testing data. For particular configurations it was observed that non-diffuse Albedo components may influence the solar gain significantly.

It can be concluded that the numerical model implemented at EMPA is suitable to calculate the solar gain of multiple glazing and louver type shading devices with non-specular surfaces. For complex constructions, i.e. ventilated double envelope façades, testing of real scale components will remain important in order to validate more detailed component modelling, which in those cases should be the basis of building simulation and design [16].

ACKNOWLEDGEMENTS

The Swiss Federal Office of Energy gave financial support for this work as a part of EMPA's involvement in Task 27 of the International Energy Agency. We acknowledge with thanks the support of R. Vonbank, R. Blessing and S. Carl in mounting the experimental set-up and operating the data acquisition system.

REFERENCES

[1] H. Simmler, B. Binder, R. Vonbank, Wärmelasten transparenter Bauteile und Sonnenschutzsysteme, Final Report EMPA/BFE, Dübendorf, 2000 (in German).

[2] International Energy Agency (IEA), Solar Heating and Cooling Programme, Task 27: "Performance of Solar Façade Components", see www.iea-shc-task27.org.

[3] EN ISO 15099 (2003): Thermal performance of windows, doors and shading devices - Detailed calculations.

[4] H. Manz et al., Air flow patterns and thermal behavior of mechanically ventilated glass double façades, Building and Environment 39 (2004) 1023 – 1033.

[5] W.J. Platzer, Testing considerations for solar shading systems, IEA Task 27 working document, 2002.

[6] EN 410 (1998): Glass in building - Determination of luminous and solar characteristics of glazing.

[7] EN 13363-1 (2003) / prEN 13363-2: Solar protection devices combined with glazing, Calculation of solar and light transmittance, Part 1: Simplified method / Part 2: Detailed calculation method.

[8] R. Siegel, J.R. Howell, Thermal radiation heat transfer, Mc-Graw-Hill Inc., New York, 1972.

[9] T.E. Kuhn et al., Evaluation of overheating protection with sun-shading systems, Solar Energy 69, pp. 59 – 74, 2000.

[10] R. Perez, R. Stewart, Solar irradiance conversion models, Solar Cells Vol. 18, 1986, pp. 213-222.

[11] H. Simmler, B. Binder, Determination of the angular-dependent solar heat gain of glazing with exterior Venetian blind shading, Proc. Int. Conf. on Dynamic Analysis and Modelling to Energy Performance Assessment and Prediction of Buildings and Components, JRC Ispra, 2003.

[12] B. Binder, EMPA report 860'065, Work Package 3, Round robin tests as feasibility study for standardization, EN-Project No NNE5-1999-0511, March 2003.

[13] LORD 2.3, Developer O. Gutschker, Technical University Cottbus, 2003.

[14] H. Simmler, Messung und Simulation von transparenten Bauteilen mit Sonnenschutz, Final Report EMPA/BFE, Dübendorf, 2005 (in German).

[15] W.J. Platzer, Performance assessment for solar shading devices – state of the art, Proceedings IEA Task 27 Dissemination Workshop, Freiburg, Germany, 2003.

[16] H. Manz, T. Frank, Thermal simulation of buildings with double-skin façades, Energy & Buildings, submitted 2004.